

Article

Local Stability Analysis of a Thermo-Economic Model of a Chambadal-Novikov-Curzon-Ahlborn Heat Engine

Marco A. Barranco-Jiménez¹, Ricardo T. Páez-Hernández², Israel Reyes-Ramírez^{3,*} and Lev Guzmán-Vargas³

¹ Departamento de Formación Básica, Escuela Superior de Cómputo del IPN, Av. Miguel Bernard Esq. Juan de Dios Bátiz, U.P. Zacatenco, México D.F. 07738, México; E-Mail: mbarrancoj@ipn.mx

² Área de Física de Procesos Irreversibles, Departamento de Ciencias Básicas, Universidad Autónoma Metropolitana Azcapotzalco, Av. San Pablo 180, Col. Reynosa Tamps., México D.F. 02200, México; E-Mail: phrt@correo.azc.uam.mx

³ Unidad Profesional Interdisciplinaria en Ingeniería y Tecnologías Avanzadas del IPN, Av. IPN 2580, L. Ticomán, México D.F. 07340, México; E-Mail: lguzmanv@ipn.mx

* Author to whom correspondence should be addressed; E-Mail: ireyesr@ipn.mx; Tel.: +52-55-57296000 ext. 56873; Fax: +52-55-57529318.

Received: 29 June 2011; in revised form: 3 August 2011 / Accepted: 17 August 2011 /

Published: 29 August 2011

Abstract: In this work we present a local stability analysis of the thermo-economic model of an irreversible heat engine working at maximum power conditions. The thermo-economic model is based on the maximization of a benefit function which is defined by the ratio of the power output and the total cost involved in the plant's performance. Our study shows that, after a small perturbation, the system decays exponentially to the steady state determined by two different relaxation times. In particular, we show that the relaxation times are function of the temperature ratio $\tau = T_2/T_1$ ($T_1 > T_2$), the cost function f and the parameter R (a parameter related to the degree of internal irreversibilities). We observe that the stability of the system improves as τ increases whereas for changes in f and R , the stability properties are characterized by a rapid decay along the fast eigendirection as f increases and R decreases. Finally, we discuss our results in the context of energetic properties.

Keywords: thermo-economics; local stability; endoreversible heat engine

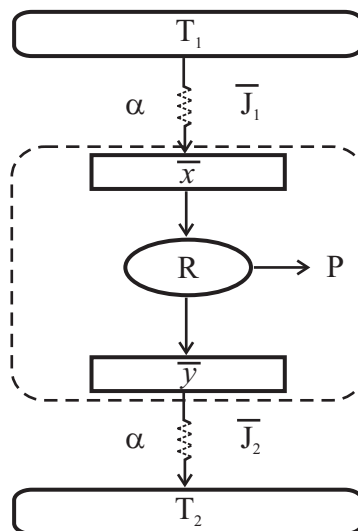
1. Introduction

During the last decades, since the early work by Curzon and Ahlborn was published [1], most of the studies of Finite-Time Thermodynamics (FTT) have focused on steady-state energetic properties [2–10]. However, it is important to notice that any thermal engine is exposed to continuous internal and external perturbations while operating. In order to have a well-designed system, it is important to analyze the effect of noisy perturbations on the stability of the system steady state. This analysis may allow us to guarantee proper dynamical behavior of the system like stability and small relaxation times, or to warn about possible failure in the performance of a thermal engine. In 2001, Santillán *et al.* [11] studied the local stability analysis of an endoreversible Curzon-Ahlborn heat engine operating under maximum power conditions. Later, Guzmán-Vargas *et al.* [12] investigated the effect of the heat transfer laws and the thermal conductances on the local stability of an endoreversible heat engine. Recently, Páez-Hernández *et al.* [13], analyzed the local stability of a non-endoreversible Curzon-Ahlborn engine taking into account the engines implicit time delays operating at maximum power regime. However, the local stability analyses described above have not considered the effect of economical aspects. Within the context of Finite-Time Thermodynamics [2–5,7], the effect of economical aspects was early introduced by De Vos [14] for the study of a thermo-economic model of a power plant [15–17]. Later, and in the same direction, Sahin and Kodal [18] studied the thermo-economics of an endoreversible heat engine in terms of the maximization of a profit function defined as the quotient of the power output and the annual investment and the full consumption costs. This thermo-economic performance analysis [16,17,19] consists in maximizing a benefit function in terms of the power output and the cost involved in the performance of the power plant [20–24]. The aim of this paper is to extend the local stability analysis of the Chambadal-Novikov-Curzon-Ahlborn (CNCA) heat engine model [1,15,25], by considering a Newton heat transfer law as well as to analyze the effect of internal irreversibilities and economical aspects. The paper is organized as follows: In Section 2, we present the thermo-economical analysis of a non-endoreversible CNCA heat engine. In Section 3, we describe the local stability analysis method applied to a two-dimensional system. In Section 4, the local stability analysis of a CNCA heat engine is presented. Finally, in Section 5, we present our conclusions.

2. Thermo-Economic Analysis of the Steady-State Chambadal-Novikov-Curzon-Ahlborn Heat Engine

In this section, we review the thermo-economic analysis of a non-endoreversible Novikov-Curzon-Ahlborn heat engine. A schematic diagram of the CNCA engine is shown in Figure 1. This engine consists in a Carnot-like thermal engine that works in irreversible cycles and exchanges heat with external thermal reservoirs at temperatures T_1 and T_2 ($T_1 > T_2$). In the steady state, the temperatures of the Carnot-like cycle isothermal branches are \bar{x} and \bar{y} , here overbars are used to indicate the corresponding steady-state values. The steady-state heat flows between thermal reservoirs and working fluid \bar{J}_1 and \bar{J}_2 are also show in Figure 1.

Figure 1. Schematic representation of a non-endoreversible Curzon-Ahlborn engine.



By applying the Clausius theorem and using the fact that the inner Carnot-like engine works in irreversible cycles, we get the following inequality

$$\frac{\bar{J}_1}{\bar{x}} - \frac{\bar{J}_2}{\bar{y}} < 0 \tag{1}$$

this expression can be transformed into an equality by introducing a parameter R , leading to

$$\frac{\bar{J}_1}{\bar{x}} = R \frac{\bar{J}_2}{\bar{y}} \tag{2}$$

The parameter R , which in principle is within the interval $0 \leq R \leq 1$ ($R = 1$ corresponds to the endoreversible limit), can be seen as a measure of the departure from the endoreversible regime [26–28]. If we assume that the heat flows from T_1 to \bar{x} and from \bar{y} to T_2 are of the Newton type, then

$$J_1 = \alpha(T_1 - \bar{x}) \tag{3}$$

$$J_2 = \alpha(\bar{y} - T_2) \tag{4}$$

where α is the thermal conductance. For simplicity of calculations, we have assumed that the heat exchanges take place in conductors with the same thermal conductance α . The systems steady-state power output and the efficiency can be defined as

$$\bar{P} = \bar{J}_1 - \bar{J}_2 \tag{5}$$

and

$$\bar{\eta} = \frac{\bar{P}}{\bar{J}_1} = 1 - \frac{\bar{J}_2}{\bar{J}_1} = 1 - \frac{1}{R} \frac{\bar{y}}{\bar{x}} \tag{6}$$

By combining Equations (2), (4) and (6), we can write \bar{x} and \bar{y} as

$$\bar{x} = \frac{T_1}{1 + R} \left(1 + \frac{\tau}{1 - \bar{\eta}} \right) (1 - \bar{\eta}) \tag{7}$$

$$\bar{y} = \frac{R}{1 + R} T_1 \left(1 + \frac{\tau}{1 - \bar{\eta}} \right) (1 - \bar{\eta}) \tag{8}$$

where $\tau = T_2/T_1$. De Vos thermo-economical analysis considers a profit function \bar{F} , which is maximized [14]. This profit function is given by the quotient of the power output \bar{P} and the total cost involved in the performance of the power plant \bar{C}_{tot} ,

$$\bar{F} = \frac{\bar{P}}{\bar{C}_{tot}} \tag{9}$$

In his study, De Vos assumed that the running costs of the plant consist in two parts: a capital cost which is proportional to the investment and, therefore, to the size of the plant and, a fuel cost that is proportional to the fuel consumption and, therefore, to the heat input rate. Assuming that is an appropriate measure for the size of the plant, the running cost of the plant exploitation is defined as [14]

$$\bar{C}_{tot} = a\bar{J}_{max} + b\bar{J}_1 = a\alpha T_1 \left[(1 - \tau) + \beta \left(1 - \frac{\bar{x}}{T_1} \right) \right] \tag{10}$$

where the proportionality constants a and b have units of $\$/Joule$, $\beta = b/a$ and $\bar{J}_{max} = \alpha(T_1 - T_2)$ is the maximum heat that can be extracted from the heat reservoir without supplying work (see Figure 1). By using Equations (4), (6), (7), (9) and (10), the profit function can be written as,

$$a\bar{F} = \bar{\eta} \frac{\frac{1}{1 + R} \left(R - \frac{\tau}{1 - \bar{\eta}} \right)}{(1 - \tau) + \frac{\beta}{1 + R} \left(R - \frac{\tau}{1 - \bar{\eta}} \right)} \tag{11}$$

If we calculate the derivative of $a\bar{F}$ with respect to $\bar{\eta}$, we can determine the efficiency that maximizes \bar{F} by $\left(\frac{d(a\bar{F})}{d\bar{\eta}} \right)_{\bar{\eta}=\bar{\eta}^*} = 0$ [29], and then we obtain

$$\bar{\eta}^*(\beta, \tau, R) = 1 - \sqrt{\frac{\tau}{R} \frac{R(1 - \tau) - \tau\beta}{R(1 - \tau)\sqrt{1 + \frac{\beta(R - \tau)}{R(1 - \tau)}} - \sqrt{R\tau\beta}}} \tag{12}$$

For $R = 1$ the result for the efficiency previously obtained by De Vos is recovered [14,30,31]. Besides, when $\beta = 0$, we obtain $\eta = 1 - \sqrt{\frac{\tau}{R}}$, which was previously obtained by Wu and Kiang [26], and by Arias-Hernández *et al.* [32]. Now, we consider the fractional fuel cost defined by [14]

$$f = \frac{\bar{J}_1\beta}{\bar{J}_{max} + \bar{J}_1\beta} \tag{13}$$

that is, the ratio of the fuel cost and the total cost of the plant [14]. This parameter is related to several energy resources, taking into account energy sources where the investment is the preponderant cost ($f = 0$) up to energy sources where the fuel is the predominant cost ($f = 1$). This new parameter allows the efficiency and the power output to be expressed as

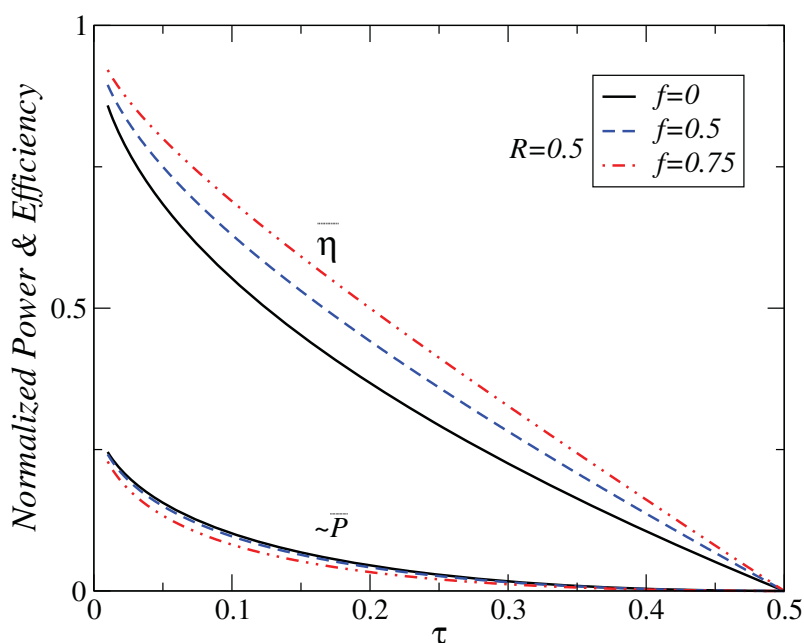
$$\bar{\eta}^*(f, \tau, R) = 1 - \frac{f}{2R}\tau - \frac{\sqrt{4(1 - f)\tau R + f^2\tau^2}}{2R} \tag{14}$$

and

$$\bar{P} = \alpha T_1 \frac{\left[(f - 2)\tau - \sqrt{4(1 - f)\tau R + f^2\tau^2} \right] \left[f\tau - 2R + \sqrt{4(1 - f)\tau R + f^2\tau^2} \right]}{2(1 + R) \left[-f\tau - \sqrt{4(1 - f)\tau R + f^2\tau^2} \right]} \tag{15}$$

Equations (14) and (15) represent the steady-state efficiency $\bar{\eta}$ and power output \bar{P} respectively. They are functions of τ , f and R for a non-endoreversible CNCA engine working under the maximum-profit regime. It is straightforward to show that both $\bar{P}/\alpha T_1$ and $\bar{\eta}$ are decreasing functions of τ for every fixed value of R , as we can see in Figure 2.

Figure 2. Plots of normalized power output ($\bar{P}/\alpha T_1$) and efficiency ($\bar{\eta}$) versus τ , for different values of the fractional fuel cost.



3. Linearization and Stability Analysis

In this section we present a brief description of the local stability analysis for a two-dimensional system [33]. Consider the following dynamical system,

$$\frac{dx}{dt} = f(x, y) \tag{16}$$

and

$$\frac{dy}{dt} = g(x, y) \tag{17}$$

Let (\bar{x}, \bar{y}) be a fixed point such that $f(\bar{x}, \bar{y}) = 0$ and $g(\bar{x}, \bar{y}) = 0$. Consider a small perturbation around this fixed point and write $x = \bar{x} + \delta x$ and $y = \bar{y} + \delta y$, where δx and δy are small perturbations from the corresponding fixed point values. By substituting into Equations (16) and (17), expanding $f(\bar{x} + \delta x, \bar{y} + \delta y)$ and $g(\bar{x} + \delta x, \bar{y} + \delta y)$ in a Taylor series, and using the fact that δx and δy are small to neglect quadratic terms, the following equations are obtained for the perturbations,

$$\begin{pmatrix} \frac{d\delta x}{dt} \\ \frac{d\delta y}{dt} \end{pmatrix} = \begin{pmatrix} f_x & f_y \\ g_x & g_y \end{pmatrix} \begin{pmatrix} \delta x \\ \delta y \end{pmatrix} \tag{18}$$

where $f_x = \frac{\partial f}{\partial x}|_{\bar{x},\bar{y}}$; $f_y = \frac{\partial f}{\partial y}|_{\bar{x},\bar{y}}$; $g_x = \frac{\partial g}{\partial x}|_{\bar{x},\bar{y}}$ and $g_y = \frac{\partial g}{\partial y}|_{\bar{x},\bar{y}}$. Equation (18) is a linear system of differential equations. Thus, we assume that the general solution of the system is of the form,

$$\delta\vec{r} = e^{\lambda t}\vec{u} \tag{19}$$

with $\delta\vec{r} = (\delta x, \delta y)$ and $\vec{u} = (u_x, u_y)$. Substitution of solution $\delta\vec{r}$ into Equation (18) yields to the following eigenvalue equation,

$$A\delta\vec{r} = \lambda\delta\vec{r} \tag{20}$$

where A is the matrix given by the first term in the right-hand side of Equation (18). The eigenvalues of this equation are the roots of the characteristic equation,

$$|A - \lambda I| = (f_x - \lambda)(g_y - \lambda) - g_x f_y = 0 \tag{21}$$

If λ_1 and λ_2 are solutions of Equation (21), the general solution of the system is

$$\delta\vec{r} = c_1 e^{\lambda_1 t} \vec{u}_1 + c_2 e^{\lambda_2 t} \vec{u}_2 \tag{22}$$

where c_1 and c_2 are arbitrary constants and \vec{u}_1 and \vec{u}_2 are the eigenvectors corresponding to λ_1 and λ_2 , respectively. To determine \vec{u}_1 and \vec{u}_2 we use again Equation (20) for each eigenvalue. Information about the stability of the system can be obtained from the value of the eigenvalues λ_1 and λ_2 . In general, λ_1 and λ_2 are complex numbers. If both λ_1 and λ_2 have negative real parts, the fixed point is stable. Moreover, if both eigenvalues are real and negative, the perturbations decay exponentially [33]. In this last case, it is possible to identify characteristic time scales for each eigendirection as

$$t_1 = \frac{1}{|\lambda_1|} \tag{23}$$

and

$$t_2 = \frac{1}{|\lambda_2|} \tag{24}$$

4. Local Stability Analysis

Following Santillán *et al.* [11], and assuming that the working fluid at the isothermal branches x and y are not real heat reservoirs but macroscopic objects with heat capacity C , the internal temperatures x and y (see Figure 1) change according to the following differential equations

$$\frac{dx}{dt} = \frac{1}{C} [\alpha(T_1 - x) - J_1] \tag{25}$$

and

$$\frac{dy}{dt} = \frac{1}{C} [J_2 - \alpha(y - T_2)] \tag{26}$$

where J_1 and J_2 are the heat flows described in Figure 1. According to the non-endoreversibility hypothesis, J_1 and J_2 are given by

$$J_1 = \frac{Rx}{Rx - y} P \tag{27}$$

and

$$J_2 = \frac{y}{Rx - y} P \tag{28}$$

On the other hand, we can use Equations (6) and (14) to construct an expression which relates the internal variables \bar{x} and \bar{y} , to the external temperatures T_1 and T_2 , given by

$$\tau = \frac{\bar{y}^2}{\bar{x}^2(1-f)R + \bar{x}\bar{y}f} \tag{29}$$

In a similar way to Equation (29), by using Equations (7) and (14), we can obtain an expression for T_1

$$T_1 = \frac{2(f-1)(1+R)\bar{x}}{2(f-1) + \frac{f\bar{y}^2}{\bar{x}(1-f)+R\bar{x}^2+\bar{x}\bar{y}f} + \frac{2(1-f)R\bar{x}\bar{y}+\bar{y}^2f}{\bar{x}(1-f)R\bar{x}+\bar{y}f}} \tag{30}$$

The corresponding steady-state values of \bar{x} and \bar{y} as function of T_1 and T_2 at maximum-profit function are obtained by substituting Equation (14) into Equations (7) and (8), respectively

$$\bar{x} = \frac{T_1}{1+R} \left(1 + \frac{2R\tau}{f\tau + \sqrt{4(1-f)\tau R + f^2\tau^2}} \right) \tag{31}$$

and

$$\bar{y} = \frac{RT_1}{2(1+R)} \left((f+2R)\tau + f\tau + \sqrt{4(1-f)\tau R + f^2\tau^2} \right) \tag{32}$$

We can observe from Equations (29)–(32) that for the case $f = 0$ and $R = 1$, the results previously obtained by Santillán *et al.* [11] and Guzmán-Vargas *et al.* [12] are recovered. Finally, by substituting Equations (29) and (30) into Equation (15), the steady-state power output can be expressed as

$$\bar{P}(\bar{x}, \bar{y}, f, R) = \alpha \frac{\left[\bar{x}\Lambda + \frac{(f-2)\bar{x}\bar{y}^2}{(1-f)R\bar{x}+f\bar{x}\bar{y}} \right] \left[\Lambda - 2R + \frac{f\bar{y}^2}{(1-f)R\bar{x}+f\bar{x}\bar{y}} \right]}{2 \left[\Lambda + \frac{(f+2R)\bar{y}^2}{(1-f)R\bar{x}+f\bar{x}\bar{y}} \right]} \tag{33}$$

where

$$\Lambda = \sqrt{\frac{\bar{y}^2 [2(1-f)R\bar{x} + f\bar{y}^2]^2}{\bar{x}^2 [2(f-1)R\bar{x} + f\bar{y}^2]^2}} \tag{34}$$

By using the assumption [11,12] that out of the steady state but not too far away, the power output of a Curzon-Ahlborn heat engine depends on x and y in the same way that it depends on \bar{x} and \bar{y} at the steady-state ($\bar{P}(\bar{x}, \bar{y}, f, R) \rightarrow P(x, y, f, R)$), that is, this assumption is applicable only in the vicinity of the steady state, we can write the dynamical equations for x and y as follows

$$\frac{dx}{dt} = \frac{1}{C} \left[\alpha(T_1 - x) - \frac{Rx}{Rx - y} P(x, y, f, R) \right] \tag{35}$$

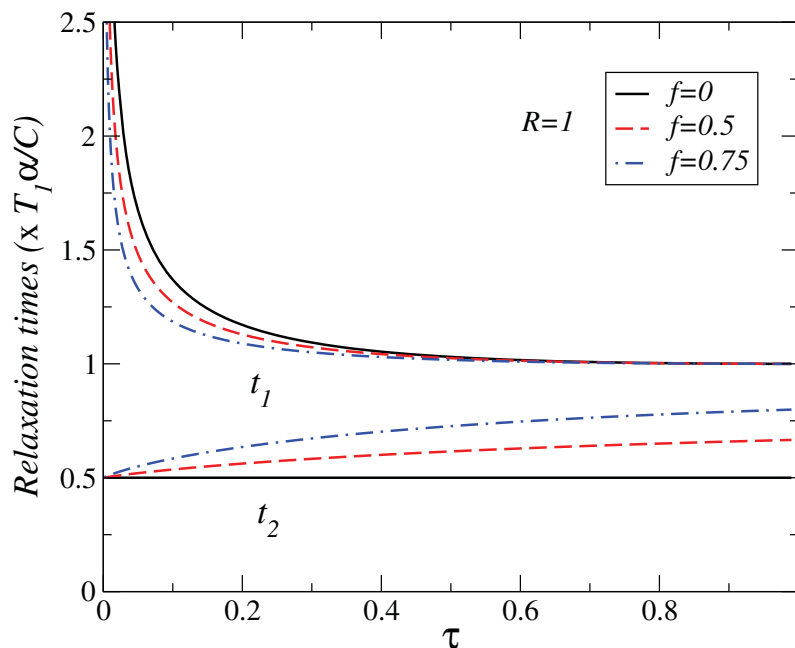
and

$$\frac{dy}{dt} = \frac{1}{C} \left[\frac{y}{Rx - y} P(x, y, f, R) - \alpha(y - T_2) \right] \tag{36}$$

To analyze the system stability near the steady state, we proceed following the steps described in the previous sections. After solving the corresponding eigenvalue equation, we find that both eigenvalues (λ_1 and λ_2) are function of α, C, τ, f and R . The final expression and the algebraic details are not shown because they are quite lengthy and can be easily reproduced with the help of a symbolic algebra package. Specifically, our calculations show that both eigenvalues are real and negative, with $\lambda_2 < \lambda_1$, and then $t_1 > t_2$, where t_1, t_2 correspond to the slow and fast eigendirection, respectively. Thus, the steady state

is stable because any perturbation would be decay exponentially. The expressions of the eigenvalues when $f = 0$ are consistent with those previously reported in [11,12]. In Figure 3, the relaxation times are plotted against τ for different values of fractional fuel cost f , for a fixed value of R ($R = 1$), that is, the endoreversible case. We observe that t_1 is a decreasing function of τ . This relaxation time decreases as the fuel cost increases, indicating a faster decay along this eigendirection as $f \rightarrow 1$.

Figure 3. Plot of relaxation times t_1, t_2 versus τ for several values of the fractional fuel cost f in the endoreversible case ($R = 1$).



For t_2 , we observe that this relaxation time remains constant as τ increases for $f = 0$. As the fractional fuel cost f increases, t_2 slightly increases too. We notice that in the limit $f \rightarrow 1$, both relaxation times tend to be closer each other, indicating that the stability is preserved for values within the interval $0 < \tau < 1$. In Figure 4 we also show the relaxation times as a function of τ , for several values of the parameter R , for a fixed value of the fractional fuel cost f . As in Figure 3, t_1 is a decreasing function of τ . We observe that t_2 remains almost constant and slightly increases when the irreversibility parameter changes. From the findings of Figures 3 and 4, we can conclude that the system is stable for $\tau > 0$. We remark that as the fractional fuel cost f increases, t_1 decreases whereas t_2 varies smoothly, for a given value of R . Likewise, for a given value of f , as the irreversibility parameter R decreases, t_1 decreases whereas t_2 increases. Additionally, in Figure 5 we show the relaxation times versus fuel fractional cost for several values of τ . We can see, in this case, how the fast (slow) relaxation time slightly increases (decreases) as f changes from 0 to 1. It is important to notice that the optimal efficiency smoothly increases as f moves from 0 to 1, and we have seen that the stability is preserved for variations of f in the same range. We also remark that the power output and the efficiency depend on τ for the cases analyzed here, and both energetic quantities are decreasing functions of this parameter, that is, the systems stability moves in the opposite direction to that of the steady state P and η as τ varies.

Figure 4. Plot of relaxation times t_1, t_2 versus τ for several values of the endoreversibility parameter R and a value of the fractional fuel cost.

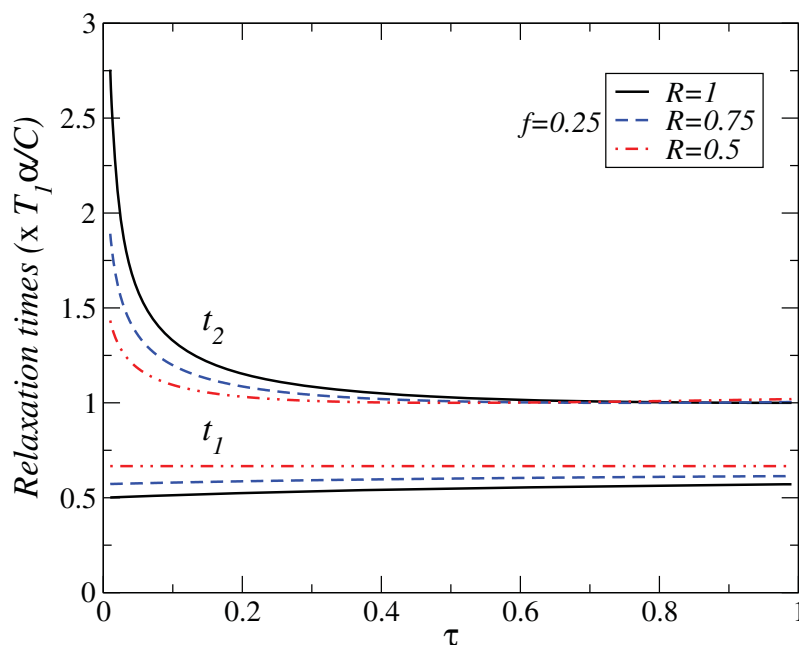
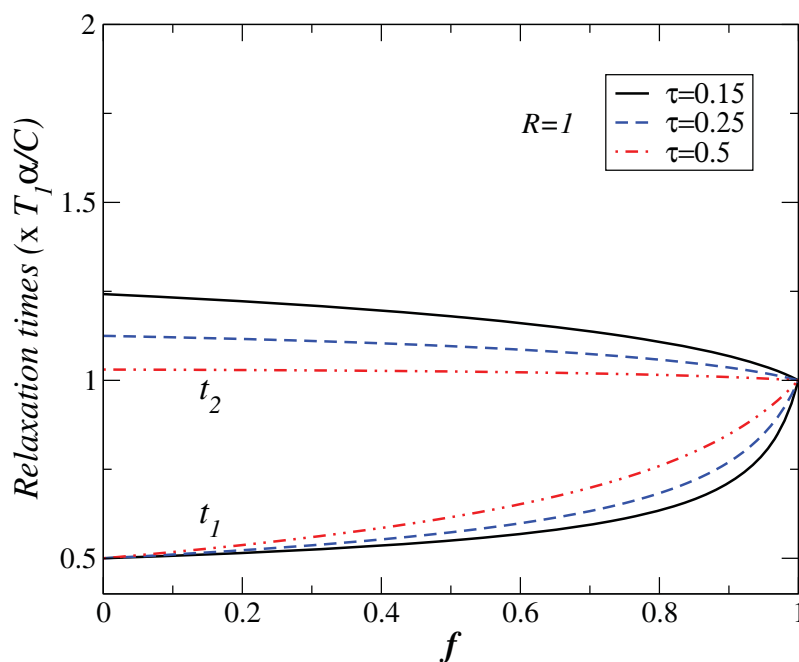


Figure 5. Relaxation times t_1, t_2 versus f for several values of τ in the endoreversible case.



5. Conclusions

A thermo-economical local stability analysis of a Novikov-Curzon-Ahlborn heat engine was proposed. We show that the relaxation times are function of α, C, τ, f and R . We have explored the dependence of the relaxation times on the economic parameter f associated to the kind of fuel used. Our findings are consistent with previous results about stability of heat engines and on the irreversibility parameter R [11–13]. After a small perturbation the system decays exponentially to the steady state determined by two different relaxation times. We have seen that the stability properties of the system are

preserved when the fractional fuel cost f moves from situations where the investment is the preponderant cost ($f = 0$) to cases where the fuel is the preponderant cost ($f = 1$). Finally, we observe that the stability of the system improves as τ increases whereas the steady-state energetic properties of the engine declines for all cases of energy resources treated here.

Acknowledgements

This work was supported in part by CONACYT, COFAA and EDI-IPN-México.

References

1. Curzon, F.; Ahlborn, B. Efficiency of a Carnot engine at maximum power output. *Am. J. Phys.* **1975**, *43*, 22–24.
2. Feidt, M.; Costea, M.; Petre, C.; Petrescu, S. Optimisation of the direct carnot cycle. *Appl. Therm. Eng.* **2007**, *27*, 829–839.
3. Feidt, M.L. Optimal use of energy system and processes. *Int. J. Exergy* **2008**, *5*, 500–531.
4. Chen, L.; Sun, F. *Advances in Finite Time Thermodynamics: Analysis and Optimization*; Nova Science: New York, NY, USA, 2004.
5. Sieniutycz, S.; Jezowski, J. *Energy Optimization in Process Systems*; Elsevier: Oxford, UK, 2009.
6. De Vos, A. *Endoreversible Thermodynamics of Solar Energy Conversion*; Oxford University Press: Oxford, UK, 1992.
7. Andresen, B. Current trends in finite-time thermodynamics. *Angew. Chem. Int. Ed.* **2011**, *50*, 2690–2704.
8. Fisher, M.; Hoffmann, K.H. Can a quantitative simulation of an Otto engine be accurately rendered by a simple Novikov model with heat leak? *J. Non-Equilib. Thermodyn.* **2004**, *29*, 9–28.
9. Velasco, S.; Roco, J.M.M.; Medina, A.; White, J.A.; Calvo-Hernández, A. Optimization of heat engines including the saving of natural resources and the reduction of thermal pollution. *J. Phys. D* **2000**, *33*, 355–359.
10. Sieniutycz, S.; Salamon, P. *Finite Time Thermodynamics and Thermoconomics*; Taylor and Francis: London, UK, 1990.
11. Santillán, M.; Maya-Aranda, G.; Angulo-Brown, F. Local stability analysis of an endoreversible Curzon-Ahlborn-Novikov engine working in a maximum-power like regime. *J. Phys. D* **2001**, *34*, 2068–2072.
12. Guzmán-Vargas, L.; Reyes-Ramírez, I.; Sánchez-Salas, N. The effect of heat transfer laws and thermal conductances on the local stability of an endoreversible heat engine. *J. Phys. D* **2005**, *38*, 1282–1291.
13. Páez-Hernández, R.T.; Angulo-Brown, F.; Santillán, M. Dynamic robustness and thermodynamic optimization in a non-endoreversible curzonAhlborn engine. *J. Non-Equilib. Thermodyn.* **2006**, *31*, 173–188.
14. De Vos, A. Endoreversible thermoconomics. *Energy Convers. Manage.* **1995**, *36*, 1–5.
15. Novikov, I.I. The efficiency of atomic power stations (a review). *At. Energ.* **1957**, *3*, 409.

16. Qin, X.; Chen, L.; Sun, F.; Wu, C. Thermo-economic optimization of an endoreversible four-heat-reservoir absorption-refrigerator. *Appl. Energy* **2005**, *81*, 420–433.
17. Chen, L.; Sun, F.; Wu, C. Endoreversible thermo-economics for heat engines. *Appl. Energy* **2005**, *81*, 388–396.
18. Sahin, B.; Kodal, A. Performance analysis of an endoreversible heat engine based on a new thermo-economic optimization criterion. *Energy Convers. Manage.* **2001**, *3*, 1085–1093.
19. Wu, C.; Chen, L.; Chen, J. *Recent Advances in Finite-Time Thermodynamics*; Nova Science: New York, NY, USA, 1999.
20. Barranco-Jiménez, M.A.; Sánchez-Salas, N.; Angulo-Brown, F. Finite-time thermo-economic optimization of a solar-driven heat engine model. *Entropy* **2011**, *13*, 171–183.
21. Wu, F.; Wu, C.; Guo, F.; Li, Q.; Chen, L. Optimization of a thermoacoustic engine with a complex heat transfer exponent. *Entropy* **2003**, *5*, 444–451.
22. Zheng, T.; Chen, L.; Sun, F.; Wu, C. Effect of heat leak and finite thermal capacity on the optimal configuration of a two-heat-reservoir heat engine for another linear heat transfer law. *Entropy* **2003**, *5*, 519–530.
23. Chen, L.; Zheng, T.; Sun, F.; Wu, C. Optimal cooling load and COP relationship of a four-heat-reservoir endoreversible absorption refrigerator cycle. *Entropy* **2004**, *6*, 316–326.
24. Barranco-Jimenez, M.A.; Sanchez-Salas, N.; Rosales, M.A. Thermo-economic optimum operation conditions of a solar-driven heat engine model. *Entropy* **2009**, *11*, 443–453.
25. Chambadal, P. *Les Centrales Nucléaires*; Armand Colin: Paris, France, 1957.
26. Wu, C.; Kiang R.L. Finite-time thermodynamic analysis of a Carnot engine with internal irreversibility. *Energy* **1992**, *1*, 1173–1178.
27. Chen, J. The maximum power output and maximum efficiency of an irreversible Carnot heat engine. *J. Phys. D* **1994**, *27*, 1144–1149.
28. Ozcaynak, S.; Goktan, S.; Yavuz, H. Finite-time thermodynamics analysis of a radiative heat engine with internal irreversibility. *J. Phys. D* **1994**, *27*, 1139–1143.
29. Barranco-Jiménez, M.A. Finite-time thermodynamics optimization of a non endoreversible heat engine. *Rev. Mex. Fis.* **2009**, *55*, 211–220.
30. Barranco-Jiménez, M.A.; Angulo-Brown, F. Thermo-economical optimization of an endoreversible power plant model. *Rev. Mex. Fis.* **2005**, *51*, 49–56.
31. Barranco-Jiménez, M.A.; Angulo-Brown, F. Thermo-economic optimization of a Novikov power plant model under maximum ecological conditions. *J. Energy Inst.* **2007**, *80*, 96–104.
32. Arias-Hernández, L.A.; de Parga, G.A.; Angulo-Brown, F. On Some Nonendoreversible engine models with Nonlinear heat transfer laws. *Open Sys. Inf. Dyn.* **2003**, *10*, 351–375.
33. Strogatz, S.H. *Nonlinear Dynamics and Chaos with Applications to Physics, Biology, Chemistry and Engineering*; Addison-Wesley Publishing Company: Reading, MA, USA, 1994.